

22 Solving Transient Heat Conduction Problems by Means of Finite Element Method (FEM)

Theoretical fundamentals and the application of finite element method (FEM) [1–3, 6, 7, 9, 11–18, 20, 21] are presented in Chap. 11 for solving steady-state heat conduction problems. In this chapter, the authors discuss how FEM is applied when solving transient heat conduction problems. They also present the methods for integrating ordinary differential equation systems after time, which describe body temperature changes in nodes in the function of time and the differences between Galerkin- method-based FEM and the FEM based on the heat balance method, which was discussed in Chap. 21. Furthermore, the authors describe FEM-based finite volume method and the difference between this method and the Galerkin-method-based FEM, in which the finite elements are regarded as bodies with a lumped thermal capacity. Also the transformation of coordinates will be discussed as it facilitates the calculation of integrals in FEM. The authors also give a practical example in which FEM is used to determine transient temperature distribution in a complex-shape fin.

Exercise 22.1 Description of FEM Based on Galerkin Method Used for Solving Two-Dimensional Transient Heat Conduction Problems

Derive basic equations for FEM based on Galerkin method for solving two-dimensional transient heat conduction problems. Assume that temperature field is source-based, while the three boundary conditions (of 1st, 2nd and 3rd kind) are assigned on the body boundary. Account for the fact that the medium is anisotropic, i.e. $\lambda_x \neq \lambda_y$.

Solution

Find a solution for the transient heat conduction problem

$$c\rho \frac{\partial T}{\partial t} = \frac{\partial}{\partial x} \left(\lambda_x \frac{\partial T}{\partial x} \right) + \frac{\partial}{\partial y} \left(\lambda_y \frac{\partial T}{\partial y} \right) + \dot{q}_v \quad (1)$$

when initial condition is

$$T(x, y, t) \Big|_{t=0} = T_0(x, y) \quad (2)$$

and boundary conditions are

$$T|_{\Gamma_T} = T_b, \quad (3)$$

$$\left(\lambda_x \frac{\partial T}{\partial x} n_x + \lambda_y \frac{\partial T}{\partial y} n_y \right) \Big|_{\Gamma_q} = \dot{q}_B, \quad (4)$$

and

$$\left(\lambda_x \frac{\partial T}{\partial x} n_x + \lambda_y \frac{\partial T}{\partial y} n_y \right) \Big|_{\Gamma_a} = \alpha (T_{cz} - T|_{\Gamma_a}). \quad (5)$$

The method for calculating node temperature is very similar to the method used to calculate steady-state temperature (Ex. 11.10). Galerkin method is applied to make an approximate determination of temperature in element nodes: $T_j^e, j = 1, \dots, n$

$$\int_{\Omega^e} \left[c\rho \frac{\partial T^e}{\partial t} - \frac{\partial}{\partial x} \left(\lambda_x \frac{\partial T^e}{\partial x} \right) - \frac{\partial}{\partial y} \left(\lambda_y \frac{\partial T^e}{\partial y} \right) - \dot{q}_v \right] N_i^e(x, y) dx dy = 0, \quad (6)$$

where temperature distribution inside the element is formulated in (13), Ex. 11.10. Once similar transformations are carried out as those in Ex. 11.10, the following ordinary differential equation for temperature in node i of element e is obtained

$$\sum_{j=1}^n \left(M_{ij}^e \frac{dT_j^e}{dt} + K_{ij}^e T_j^e \right) = f_{Q,i}^e + f_{q,i}^e + f_{a,i}^e, \quad i = 1, \dots, n, \quad (7)$$

where

$$K_{ij}^e = K_{c,ij}^e + K_{a,ij}^e \quad (8)$$

$$M_{ij}^e = \int_{\Omega^e} c\rho N_i N_j dx dy. \quad (9)$$

The remaining terms in (7) are defined in Ex. 11.10. Matrix $[M]$ is usually called the *thermal capacity matrix* or *mass matrix*.

The elements of the capacity matrix

$$[M^e] = \int_{\Omega^e} c\rho [N]^T [N] dx dy \quad (10)$$

can be determined by means of (9) once the dependence on the shape function presented in Ex. 11.9, is employed. For a rectangular element, matrix $[M^e]$ has the form

$$[M^e] = \int_{\Omega^e} c\rho [N]^T [N] dx dy = \int_{\Omega^e} c\rho \begin{bmatrix} (N_1^e)^2 & N_1^e N_2^e & N_1^e N_3^e & N_1^e N_4^e \\ N_1^e N_2^e & (N_2^e)^2 & N_2^e N_3^e & N_2^e N_4^e \\ N_1^e N_3^e & N_2^e N_3^e & (N_3^e)^2 & N_3^e N_4^e \\ N_1^e N_4^e & N_2^e N_4^e & N_3^e N_4^e & (N_4^e)^2 \end{bmatrix} dx dy. \quad (11)$$

Once calculations are carried out the way they were in Ex. 11.11, the following thermal capacity matrix is obtained

$$[M^e] = c\rho \frac{A^e}{36} \begin{bmatrix} 4 & 2 & 1 & 2 \\ 2 & 4 & 2 & 1 \\ 1 & 2 & 4 & 2 \\ 2 & 1 & 2 & 4 \end{bmatrix}, \quad (12)$$

where A^e is the surface area of the element.

Thermal capacity matrix (10) for a triangular element has the form

$$[M^e] = \int_{\Omega^e} c\rho \begin{bmatrix} (N_1^e)^2 & N_1^e N_2^e & N_1^e N_3^e \\ N_1^e N_2^e & (N_2^e)^2 & N_2^e N_3^e \\ N_1^e N_3^e & N_2^e N_3^e & (N_3^e)^2 \end{bmatrix} dx dy. \quad (13)$$

Once calculations are carried out the way they were in Ex. 11.11, one has

$$[M^e] = c\rho \frac{A^e}{12} \begin{bmatrix} 2 & 1 & 1 \\ 1 & 2 & 1 \\ 1 & 1 & 2 \end{bmatrix}, \quad (14)$$

where A^e is the surface area of the element.

For a one-dimensional linear element, the thermal capacity matrix $[M^e]$ has the form

$$[M^e] = \int_0^L c\rho \begin{bmatrix} (N_1^e)^2 & N_1^e N_2^e \\ N_1^e N_2^e & (N_2^e)^2 \end{bmatrix} dx = \frac{c\rho L}{6} \begin{bmatrix} 2 & 1 \\ 1 & 2 \end{bmatrix}, \quad (15)$$

where L is the length of the element.

The equation system, which one can use to determine node temperature in a single element e , can be written as follows

$$[M^e] \{\dot{T}^e\} + ([K_c^e] + [K_c^\alpha]) \{T^e\} = \{f_Q^e\} + \{f_q^e\} + \{f_\alpha^e\}, \quad (16)$$

where matrixes and vectors from (16) are defined in Ex. 11.10. Symbol \dot{T} stands for $\partial T / \partial t$.

Next, one should create global equation system by summing up along the sides of (16) for all N elements, which the analyzed region was divided to. This problem is discussed in Ex. 11.15. Details regarding the formation of global equation system are also presented in Ex. 11.16–11.19.

References [1, 3–5, 7, 8, 10–12, 14, 15, 21] discuss how FEM is applied to solve transient heat conduction problems; the references also give a detailed description of the FEM method.

Exercise 22.2 Concentrated (Lumped) Thermal Finite Element Capacity in FEM

Discuss how thermal capacity is concentrated in finite elements in one, two and three-dimensional problems by assuming that linear functions are used to interpolate temperature distribution inside an element.

Solution

Ex. 11.15 presents the methods for creating global equation system in FEM. According to the second method for creating such a system, the differential equations for node i shared by element $(i-1)$ and element i (Fig. 22.1) will be written out first.

Temperature distributions in elements $(i-1)$ and i are described by functions

$$T^{i-1} = T_{i-1}N_1^{i-1} + T_iN_2^{i-1} = \frac{x_i - x}{x_i - x_{i-1}}T_{i-1} + \frac{x - x_{i-1}}{x_i - x_{i-1}}T_i, \quad x_{i-1} \leq x \leq x_i, \quad (1)$$

$$T^i = T_iN_1^i + T_{i+1}N_2^i = \frac{x_{i+1} - x}{x_{i+1} - x_i}T_i + \frac{x - x_i}{x_{i+1} - x_i}T_{i+1}, \quad x_i \leq x \leq x_{i+1}. \quad (2)$$

Differential equation for node i in the global equation system has the following form:

$$\begin{aligned} c\rho \int_{x_{i-1}}^{x_i} \frac{\partial T^{i-1}}{\partial t} N_2^{i-1} dx + c\rho \int_{x_i}^{x_{i+1}} \frac{\partial T^i}{\partial t} N_1^i dx - \lambda \int_{x_{i-1}}^{x_i} \frac{\partial^2 T^{i-1}}{\partial x^2} N_2^{i-1} dx - \\ - \lambda \int_{x_i}^{x_{i+1}} \frac{\partial^2 T^i}{\partial x^2} N_1^i dx = \int_{x_{i-1}}^{x_i} \dot{q}_v N_2^{i-1} dx + \int_{x_i}^{x_{i+1}} \dot{q}_v N_1^i dx. \end{aligned} \quad (3)$$

By substituting (1) and (2) into (3) and carrying out calculations, the equation for node i is obtained. Such equation can be also determined using the capacity matrix $[M^e]$, stiffness matrix $[K^e]$ and vector $\{f_Q^e\}$.

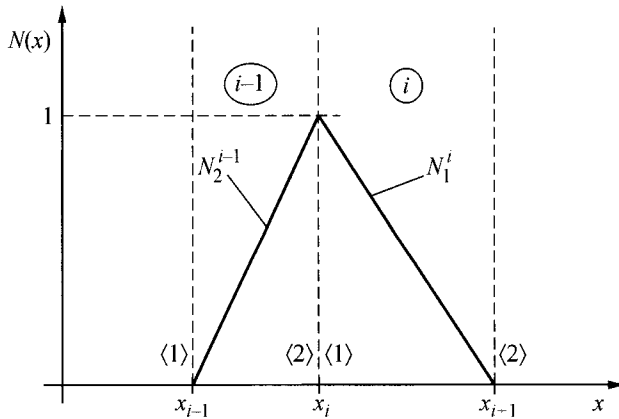


Fig. 22.1. Shape functions N_2^{i-1} i N_1^i for node i that lies on the boundary of elements $(i-1)$ and i

The local numeration of node i in the global coordinate system is number $\langle 2 \rangle$. The first term on the left-hand-side is obtained by multiplying the second row in the capacity matrix (15) by the vector of derivatives with respect to time from node temperatures, i.e.

$$\begin{aligned}
 c\rho \int_{x_{i-1}}^{x_i} \frac{\partial T^{i-1}}{\partial t} N_2^{i-1} dx &= c\rho \int_{x_{i-1}}^{x_i} \left[N_1^{i-1} N_2^{i-1}, (N_2^{i-1})^2 \right] dx \begin{Bmatrix} \dot{T}_1^{i-1} \\ \dot{T}_2^{i-1} \end{Bmatrix} = \\
 &= \frac{c\rho(x_i - x_{i-1})}{6} [1, 2] \begin{Bmatrix} \dot{T}_{i-1} \\ \dot{T}_i \end{Bmatrix} = \frac{c\rho\Delta x_{i-1}}{6} (\dot{T}_{i-1} + 2\dot{T}_i).
 \end{aligned} \tag{4}$$

The second component on the left-hand-side of (3) can be calculated in a similar way:

$$\begin{aligned}
 c\rho \int_{x_i}^{x_{i+1}} \frac{\partial T^i}{\partial t} N_1^i dx &= c\rho \int_{x_i}^{x_{i+1}} \left[(N_1^i)^2, N_1^i N_2^i \right] dx \begin{Bmatrix} \dot{T}_1^i \\ \dot{T}_2^i \end{Bmatrix} = \\
 &= \frac{c\rho(x_{i+1} - x_i)}{6} [2, 1] \begin{Bmatrix} \dot{T}_i \\ \dot{T}_{i+1} \end{Bmatrix} = \frac{c\rho\Delta x_i}{6} (2\dot{T}_i + \dot{T}_{i+1}).
 \end{aligned} \tag{5}$$

The third term on the left-hand-side is obtained by multiplying the second row in the rigidity matrix

$$[K^e] = \frac{\lambda}{L} \begin{bmatrix} 1 & -1 \\ -1 & 1 \end{bmatrix} \tag{6}$$

for a one-dimensional element by the temperature vector in the nodes of element $(i-1)$

$$-\lambda \int_{x_{i-1}}^{x_i} \frac{\partial^2 T^{i-1}}{\partial x^2} N_2^{i-1} dx = \frac{\lambda}{L^{i-1}} [-1, 1] \begin{Bmatrix} T_{i-1} \\ T_i \end{Bmatrix} = \frac{\lambda}{\Delta x_{i-1}} (-T_{i-1} + T_i). \tag{7}$$

The fourth term on the left-hand-side is obtained as a result of multiplying the first row vector in the stiffness matrix $[K^e]$ formulated in (6) by the temperature vector in nodes of element i

$$-\lambda \int_{x_i}^{x_{i+1}} \frac{\partial^2 T^i}{\partial x^2} N_1^i dx = \frac{\lambda}{L^i} [1, -1] \begin{Bmatrix} T_1^i \\ T_2^i \end{Bmatrix} = \frac{\lambda}{\Delta x_i} (T_i - T_{i+1}), \tag{8}$$

where $\Delta x_{i-1} = x_i - x_{i-1}$, $\Delta x_i = x_{i+1} - x_i$. Accounting that vector $\{f_Q^e\}$ for a one-dimensional element and linear shape functions has the form

$$\{f_Q^e\} = \frac{\dot{q}_v L}{2} \begin{Bmatrix} 1 \\ 1 \end{Bmatrix} \tag{9}$$

the terms on the right-hand-side can be expressed as follow:

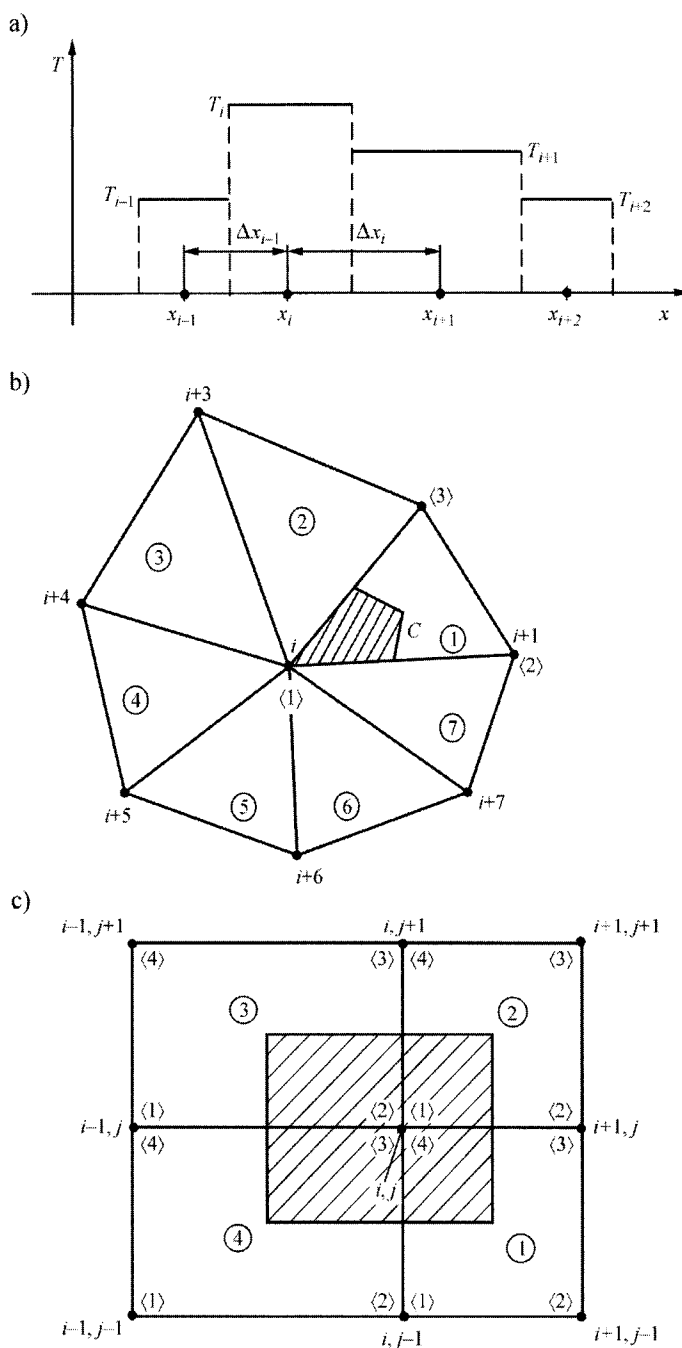


Fig. 22.2. Diagrams that illustrate the concentration of thermal capacity in node i of a) one-dimensional elements, b) two-dimensional triangular elements, c) two-dimensional tetragonal elements

$$\int_{x_{i-1}}^{x_i} \dot{q}_v N_2^{i-1} dx + \int_{x_i}^{x_{i+1}} \dot{q}_v N_1^i dx = \frac{\dot{q}_v \Delta x_{i-1}}{2} + \frac{\dot{q}_v \Delta x_i}{2}. \quad (10)$$

By accounting for (4), (5), (7), (8) and (10) in (3) one has

$$\begin{aligned} & \frac{c\rho}{6} \left[\Delta x_{i-1} (\dot{T}_{i-1} + 2\dot{T}_i) + \Delta x_i (2\dot{T}_i + \dot{T}_{i+1}) \right] - \\ & - \frac{\lambda}{\Delta x_{i-1}} (T_{i-1} - T_i) - \frac{\lambda}{\Delta x_i} (T_{i+1} - T_i) = \frac{\dot{q}_v}{2} (\Delta x_{i-1} + \Delta x_i). \end{aligned} \quad (11)$$

For equal element lengths, when $\Delta x_{i-1} = \Delta x_i = \Delta x$, (11) can be written in the form

$$\frac{c\rho\Delta x}{6} (\dot{T}_{i-1} + 4\dot{T}_i + \dot{T}_{i+1}) - \lambda \frac{T_{i-1} - 2T_i + T_{i+1}}{\Delta x} = \dot{q}_v \Delta x. \quad (12)$$

From the analysis of (12) it follows that the derivatives after time from temperatures in three nodes appear on the left-hand-side of the equation. Nodes $(i-1)$ and $(i+1)$ located next to node i , which has the largest weight equal to $4/6$, weigh $1/6$. Thermal capacity concentration (lumping) is based on the assumption that the temperature change rate in all three nodes is equal (Fig. 22.2a), i.e.

$$\dot{T}_{i-1} = \dot{T}_i = \dot{T}_{i+1}. \quad (13)$$

By accounting for this assumption in (12), one has

$$c\rho\Delta x \frac{dT_i}{dt} = \lambda \frac{T_{i-1} - 2T_i + T_{i+1}}{\Delta x} + \dot{q}_v \Delta x. \quad (14)$$

Identical equation is obtained when the straight line method, characterized by a very good accuracy, is applied.

If we assume that temperature change rates in all element nodes are identical, then the forms of thermal capacity matrixes are simplified as follow:

- one-dimensional element

$$[M^e] = \frac{c\rho L^e}{2} \begin{bmatrix} 1 & 0 \\ 0 & 1 \end{bmatrix}, \quad (15)$$

- triangular element

$$[M^e] = \frac{c\rho A^e}{3} \begin{bmatrix} 1 & 0 & 0 \\ 0 & 1 & 0 \\ 0 & 0 & 1 \end{bmatrix}, \quad (16)$$

• tetragonal element

$$[M^e] = \frac{c\rho A^e}{4} \begin{bmatrix} 1 & 0 & 0 & 0 \\ 0 & 1 & 0 & 0 \\ 0 & 0 & 1 & 0 \\ 0 & 0 & 0 & 1 \end{bmatrix}. \quad (17)$$

In each of the elements with common node i , one can single out a region with constant temperature change rate \dot{T}_i^e that can be subsequently used to calculate heat accumulation. In the case of a one-dimensional element, the length of the region measures $L^e/2$. For a triangular element, the surface area is $A^e/3$, while in the case of the tetragonal element, the surface area is $A^e/4$ (Fig. 22.2). In the global equation system for the entire region, in the equation for node i , a term appears on the left-hand-side of the equation that describes thermal changes in time of the heat accumulated within the region that can be assigned to node i . In the case of a one-dimensional problem, such region measures in width $(\Delta x_{i-1}/2 + \Delta x_i/2)$. If node i is surrounded by triangular elements (Fig. 22.2b), then temperature change rate dT_i/dt in region $1/3 \sum_{j=1}^{Ne} A^j$ is equal. Symbol Ne stands for the number of

triangular elements, which share common node i . In a case when the region is divided into tetragonal elements, the region with an equal temperature change rate is formed by summing up $1/4$ of the elements surface area with common node i (Fig. 22.2c). It is evident, therefore, that the change in heat quantity Q_{ok} in time within the control volume, whose surface is $1/4 \sum_{j=1}^{Ne} A^j$ is expressed as (Fig. 22.2c)

$$\frac{dQ_{ok}}{dt} = \frac{1}{4} \sum_{j=1}^{Ne} A^j c\rho \frac{dT_i}{dt}. \quad (18)$$

One should add that the procedure in the finite volume method (control) is identical to the procedure discussed above, as one assumes that temperature change rate is constant within the entire control volume and equals dT/dt , where i is the node that lies inside the finite volume and is assigned to this volume. Concentrating thermal capacity of a control area in a single node has its advantages; it facilitates calculations and enables one to

integrate the global system of ordinary differential equations, which define temperatures in element nodes with a larger time step Δt . Thermal capacity concentration does not decrease the accuracy of FEM, but rather it increases calculation stability.

Exercise 22.3 Methods for Integrating Ordinary Differential Equations with Respect to Time Used in FEM

Describe basic integration methods for a global ordinary differential equation system with respect to time. Such system is obtained in a semi-discrete FEM by dividing a region into finite elements.

Solution

If a differential equation system is known for an individual element (16) presented in Ex. 22.1, one can create a global equation system the way it is described in Ex.11.15. Global ordinary differential equation system for node temperature has the form

$$\mathbf{M}\dot{\mathbf{T}} + \mathbf{K}\mathbf{T} = \mathbf{F}, \quad (1)$$

where,

$$\mathbf{M} = [\mathbf{M}] = \sum_{e=1}^N [\mathbf{M}^e], \quad (2)$$

$$\mathbf{K} = [\mathbf{K}] = \sum_{e=1}^N \left([\mathbf{K}_c^e] + [\mathbf{K}_\alpha^e] \right), \quad (3)$$

$$\mathbf{F} = \{f_Q\} + \{f_q\} + \{f_\alpha\}, \quad (4)$$

$$\dot{\mathbf{T}} = [\dot{T}_1, \dots, \dot{T}_N]^T, \quad (5)$$

$$\mathbf{T} = [T_1, \dots, T_N]^T, \quad (6)$$

where N is the node number in the entire analyzed region.

Capacity matrix $[\mathbf{M}^e]$ is discussed in Ex. 22.1 and Ex. 22.2, while stiffness matrixes $[\mathbf{K}_c^e]$ and $[\mathbf{K}_\alpha^e]$ and vectors $\{f_Q\}$, $\{f_q\}$ and $\{f_\alpha\}$ are determined for different elements and boundary conditions in Ex. 11.11–11.15. A generalized Crank-Nicolson method, also known as *θ method*, will be applied to numerically integrate the equation system.

Between the temperatures in time t^{n+1} and $t^n = n\Delta t$, $n = 0, 1, \dots$ the following relation occurs

$$\mathbf{T}^{n+1} = \mathbf{T}^n + \left[(1-\theta)\dot{\mathbf{T}}^n + \theta\dot{\mathbf{T}}^{n+1} \right] \Delta t, \quad (7)$$

where $0 \leq \theta \leq 1$.

Equation (7) is known as a *generalized trapezoidal approximation*. The global equation system (1) will be written for t^{n+1} and t^n first

$$\mathbf{M}\dot{\mathbf{T}}^{n+1} + \mathbf{K}\mathbf{T}^{n+1} = \mathbf{F}^{n+1}, \quad (8)$$

$$\mathbf{M}\dot{\mathbf{T}}^n + \mathbf{K}\mathbf{T}^n = \mathbf{F}^n. \quad (9)$$

The first equation system should be multiplied on both sides by θ , while the second by $(1-\theta)$

$$\theta(\mathbf{M}\dot{\mathbf{T}}^{n+1} + \mathbf{K}\mathbf{T}^{n+1}) = \theta\mathbf{F}^{n+1}, \quad (10)$$

$$(1-\theta)(\mathbf{M}\dot{\mathbf{T}}^n + \mathbf{K}\mathbf{T}^n) = (1-\theta)\mathbf{F}^n. \quad (11)$$

By adding the sides of (10) and (11), one has

$$\mathbf{M}[(1-\theta)\dot{\mathbf{T}}^n + \theta\dot{\mathbf{T}}^{n+1}] + \mathbf{K}[(1-\theta)\mathbf{T}^n + \theta\mathbf{T}^{n+1}] = (1-\theta)\mathbf{F}^n + \theta\mathbf{F}^{n+1}, \quad (12)$$

while after allowing for (7), the equation has the form

$$\mathbf{M}\frac{\mathbf{T}^{n+1} - \mathbf{T}^n}{\Delta t} + \mathbf{K}[(1-\theta)\mathbf{T}^n + \theta\mathbf{T}^{n+1}] = (1-\theta)\mathbf{F}^n + \theta\mathbf{F}^{n+1}. \quad (13)$$

As a result of simple transformations of (13), one has

$$\left(\frac{1}{\Delta t}\mathbf{M} + \theta\mathbf{K} \right) \mathbf{T}^{n+1} = \left[\frac{1}{\Delta t}\mathbf{M} - (1-\theta)\mathbf{K} \right] \mathbf{T}^n + (1-\theta)\mathbf{F}^n + \theta\mathbf{F}^{n+1}. \quad (14)$$

If $\theta \geq 1/2$, then the solution stability is ensured for the arbitrary time step Δt . However, time step Δt should be small due to the accuracy of temperature determination. Depending on the value of parameter θ , the following methods are obtained:

- $\theta = 0$ – explicit method; it is stable under the condition that time step Δt is smaller than the reliable boundary value,
- $\theta = 1/2$ – Crank-Nicolson method, which is unconditionally stable,
- $\theta = 2/3$ – Galerkin method, which is unconditionally stable,
- $\theta = 1$ – implicit method, which is unconditionally stable.

Explicit method ($\theta = 0$) ensures high calculation accuracy with a small time step. The smaller the quotient A''/a is, the smaller the time step should be. The accuracy order of the explicit method is 1, i.e. $O(\Delta t)$. It is very easy to determine temperatures in nodes \mathbf{T}^{n+1} by means of the formula obtained from (14) with $\theta = 0$

$$\mathbf{T}^{n+1} = \mathbf{T}^n + \Delta t (\mathbf{M}^{-1} \mathbf{F}^n - \mathbf{M}^{-1} \mathbf{K} \mathbf{T}^n) \quad (15)$$

when matrix \mathbf{M} is diagonal due to the concentration (lumping) of the elements thermal capacity, and when it is easy to determine the inverse matrix \mathbf{M}^{-1} . Despite the limitations of the time step Δt , the explicit method is frequently used, since it is very accurate for a small time steps, especially when the temperature change rate for a solid is high. From the calculations in Chapter 21, one can conclude that the explicit method is no less accurate than the implicit method ($\theta = 1$) when the time step Δt is the same for both methods.

The advantage of the explicit method is that \mathbf{T}^{n+1} can be easily determined, since there is no need to solve the equation system for every time step when matrix \mathbf{M} is diagonal. Implicit method does not have this advantage, when $\theta = 1$. In the implicit method, the linear algebraic equation system must be solved at every time step by means of the direct methods, such as for e.g. Gaussian elimination method or by iterative methods, such as for example Gauss-Seidel method or over-relaxation method (SOR). The examples of solving the equation system with the implicit method are presented in Chap. 21.

Crank-Nicolson method ($\theta = 1/2$) has the second order of accuracy, i.e. $O[(\Delta t)^2]$ and is unconditionally stable. If, however, the time step Δt is too large, then the solution becomes less accurate and exhibits oscillations, which do not occur in reality. As in the case of the implicit method, the linear algebraic equation system must be solved for every time step.

Aside from the basic algorithms discussed above, which are used to solve the ordinary differential equation system, many other effective algorithms can be applied, for example. Rung-Kutt method or the algorithms of the prediction-correction type.

Exercise 22.4 Comparison of FEM Based on Galerkin Method and Heat Balance Method with Finite Volume Method

Compare different methods used for solving equations, which describe heat conduction in a flowing fluid or in a solid that flows at a velocity of $w_x = u$

$$\frac{\partial T}{\partial t} + u \frac{\partial T}{\partial x} = a \frac{\partial^2 T}{\partial x^2} + \frac{\dot{q}_v}{c\rho}. \quad (1)$$

Carry out the discretization of (1) for an internal node by means of

- FEM based on Galerkin method,
- integral heat balance method discussed in Chap. 20,
- finite volume method (finite difference method).

Also discuss thermal capacity concentration (lumping) of an element in FEM and integral heat balance method. Finite element mesh is non-uniform.

Solution

First, (1) will be discretized by means of FEM based on the Galerkin method [7] as it is done in Ex. 17.2. Once Galerkin method is applied, (1) is approximated according to FEM by means of equation

$$\begin{aligned} c\rho \int_{x_{i-1}}^{x_i} \frac{\partial T^{i-1}}{\partial t} N_2^{i-1} dx + c\rho \int_{x_i}^{x_{i+1}} \frac{\partial T^i}{\partial t} N_1^i dx + c\rho u \int_{x_{i-1}}^{x_i} \frac{\partial T}{\partial x} N_2^{i-1} dx + \\ + c\rho u \int_{x_i}^{x_{i+1}} \frac{\partial T}{\partial x} N_1^i dx - \lambda \int_{x_{i-1}}^{x_i} \frac{\partial^2 T}{\partial x^2} N_2^{i-1} dx - \lambda \int_{x_i}^{x_{i+1}} \frac{\partial^2 T}{\partial x^2} N_1^i dx = \\ = \int_{x_{i-1}}^{x_i} \dot{q}_v N_2^{i-1} dx + \int_{x_i}^{x_{i+1}} \dot{q}_v N_1^i dx. \end{aligned} \quad (2)$$

Accounting that shape functions N_1^i and N_2^{i-1} have the form

$$N_2^{i-1} = \frac{x - x_{i-1}}{x_i - x_{i-1}}, \quad N_1^i = \frac{x_{i+1} - x}{x_{i+1} - x_i} \quad (3)$$

and that temperature distribution in elements $i-1$ and i (Fig. 22.3a) is described by (1) and (2) from Ex. 22.2, from (2) one has

$$\frac{x_i - x_{i-1}}{6} (\dot{T}_{i-1} + 2\dot{T}_i) + \frac{x_{i+1} - x_i}{6} (2\dot{T}_i + \dot{T}_{i+1}) + \frac{u}{2} (T_{i+1} - T_{i-1}) + a \left(\frac{T_i - T_{i-1}}{x_i - x_{i-1}} + \frac{T_i - T_{i+1}}{x_{i+1} - x_i} \right) = \frac{x_{i+1} - x_{i-1}}{2} \frac{\dot{q}_v}{c\rho}, \quad (4)$$

where $a = \lambda/(c\rho)$. If nodes i are evenly spaced out, (4) has the form

$$\frac{\Delta x}{6} (\dot{T}_{i-1} + 4\dot{T}_i + \dot{T}_{i+1}) + \frac{u}{2} (T_{i+1} - T_{i-1}) - a \frac{T_{i-1} - 2T_i + T_{i+1}}{\Delta x} = \Delta x \frac{\dot{q}_v}{c\rho}. \quad (5)$$

Next, equations will be derived by means of FEM based on the heat balance method, which was thoroughly discussed in Chap. 20.

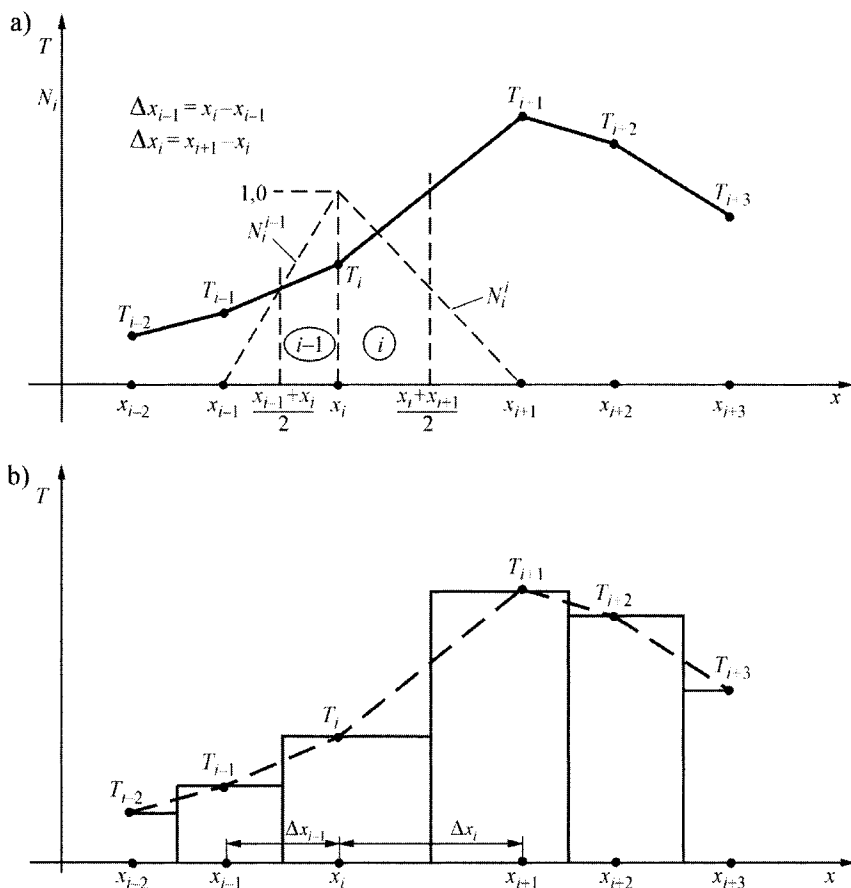


Fig. 22.3. Approximation of a one-dimensional transient temperature field at a selected moment t : a) FEM, b) finite volume method

Accounting that temperature distribution between the nodes is approximated by a straight line by means of (1) and (2) from Ex. 22.2, the heat balance equation has the form

$$\begin{aligned}
 & c\rho \int_{x_{i-1}}^{x_i} \frac{\partial T^{i-1}}{\partial t} dx + c\rho \int_{x_i}^{x_{i+1}} \frac{\partial T^i}{\partial t} dx + c\rho u \int_{x_{i-1}}^{x_i} \frac{\partial T^{i-1}}{\partial x} dx + c\rho u \int_{x_i}^{x_{i+1}} \frac{\partial T^i}{\partial x} dx - \\
 & - \lambda \int_{x_{i-1}}^{x_i} \frac{\partial^2 T^{i-1}}{\partial x^2} dx - \lambda \int_{x_i}^{x_{i+1}} \frac{\partial^2 T^i}{\partial x^2} dx = \int_{x_{i-1}}^{x_{i+1}} \dot{q}_v dx.
 \end{aligned} \quad (6)$$

Once mathematical operations are carried out, the following results are obtained:

$$\begin{aligned}
 & \frac{x_i - x_{i-1}}{8} (\dot{T}_{i-1} + 3\dot{T}_i) + \frac{x_{i+1} - x_i}{8} (3\dot{T}_i + \dot{T}_{i+1}) + \frac{u}{2} (T_{i+1} - T_{i-1}) + \\
 & + a \left(\frac{T_i - T_{i-1}}{x_i - x_{i-1}} + \frac{T_i - T_{i+1}}{x_{i+1} - x_i} \right) = \frac{x_{i+1} - x_{i-1}}{2} \frac{\dot{q}_v}{c\rho}.
 \end{aligned} \quad (7)$$

In a case when the finite element mesh is uniform, when $x_{i+1} - x_i = x_i - x_{i-1} = \Delta x$, (7) has the form

$$\frac{\Delta x}{8} (\dot{T}_{i-1} + 6\dot{T}_i + \dot{T}_{i+1}) + \frac{u}{2} (T_{i+1} - T_{i-1}) - a \frac{T_{i-1} - 2T_i + T_{i+1}}{\Delta x} = \Delta x \frac{\dot{q}_v}{c\rho}. \quad (8)$$

In the finite (control) volume method (Fig. 22.3b), the equality of temperature change rate is assumed for nodes $(i-1)$, i and $(i+1)$, i.e.

$$\frac{dT_{i-1}}{dt} = \frac{dT_i}{dt} = \frac{dT_{i+1}}{dt}. \quad (9)$$

By accounting for (9) in (7), one has

$$\begin{aligned}
 & \frac{x_{i+1} - x_{i-1}}{2} \dot{T}_i + \frac{u}{2} (T_{i+1} - T_{i-1}) + a \left(\frac{T_i - T_{i-1}}{x_i - x_{i-1}} + \frac{T_i - T_{i+1}}{x_{i+1} - x_i} \right) = \\
 & = \frac{x_{i+1} - x_{i-1}}{2} \frac{\dot{q}_v}{c\rho}.
 \end{aligned} \quad (10)$$

If the mesh is uniform, then (10) assumes the form

$$(\Delta x) \dot{T}_i + \frac{u}{2} (T_{i+1} - T_{i-1}) - a \frac{T_{i-1} - 2T_i + T_{i+1}}{\Delta x} = \Delta x \frac{\dot{q}_v}{c\rho}. \quad (11)$$

Identical equation is obtained by means of the finite difference method, if derivatives $\partial T/\partial x$ and $\partial^2 T/\partial x^2$ are approximated by central difference quotients. From the comparison of (5), (8) and (11) one can conclude that weight coefficients with \dot{T}_i are, respectively 4/6, 6/8 and 1. One can see that the smallest coefficient occurs in the Galerkin-based FEM, a slightly larger one in the FEM based on the integral balance method, while the largest one in the control volume method (of finite differences). It is easiest to solve the equations obtained from the control volume method (11) by means of the numerical methods.

The solution of the equation system (11) for all nodes enables one to accurately determine temperature distribution (Chaps. 21, 23).

Exercise 22.5 Natural Coordinate System for One-Dimensional, Two-Dimensional Triangular and Two-Dimensional Rectangular Elements

Discuss the natural coordinate system for one-dimensional elements and two-dimensional triangular and rectangular elements and linear shape functions in the natural coordinate system.

Solution

a. One-dimensional elements

In the local coordinate system (Fig. 22.4), one-dimensional temperature distribution is described by function

$$T^e = \left(1 - \frac{\bar{x}}{L}\right) T_1^e + \frac{\bar{x}}{L} T_2^e = N_1^e T_1^e + N_2^e T_2^e = \begin{bmatrix} N_1^e & N_2^e \end{bmatrix} \begin{Bmatrix} T_1^e \\ T_2^e \end{Bmatrix}. \quad (1)$$

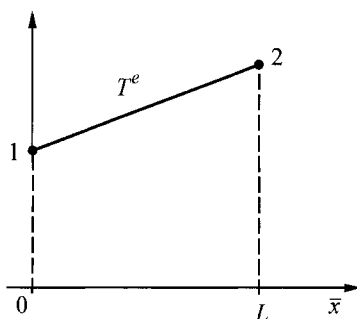


Fig. 22.4. Linear approximation of temperature distribution in the element e

Once local dimensionless coordinate system is introduced (Fig. 22.5)

$$\xi = \frac{2\bar{x}}{L} - 1, \quad (2)$$

the coordinate for node 1 is $\xi = -1$, while the coordinate for node 2 is $\xi = 1$.

Accounting for (2) in (1), one has

$$T^e = \frac{1}{2}(1-\xi)T_1^e + \frac{1}{2}(1+\xi)T_2^e = N_1^e T_1^e + N_2^e T_2^e = \begin{bmatrix} N_1^e & N_2^e \end{bmatrix} \begin{Bmatrix} T_1^e \\ T_2^e \end{Bmatrix}. \quad (3)$$

where,

$$N_1^e = \frac{1}{2}(1-\xi), \quad (4)$$

$$N_2^e = \frac{1}{2}(1+\xi) \quad (5)$$

are linear shape functions.

One should note that local coordinate \bar{x} can be expressed by means of formula

$$\bar{x} = N_1^e \bar{x}_1 + N_2^e \bar{x}_2 = \frac{1}{2}(1-\xi)\bar{x}_1 + \frac{1}{2}(1+\xi)\bar{x}_2. \quad (6)$$

Thus, (3) and (6) are very similar in form.

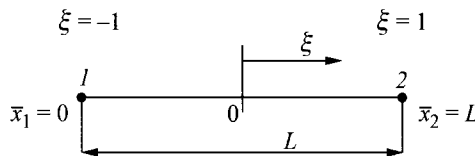


Fig. 22.5. Local dimensionless coordinate system (natural coordinate system)

b. Two-dimensional tetragonal elements

Local dimensional and dimensionless coordinate systems (natural) are presented in Fig. 22.6. If natural coordinates are introduced

$$\xi = \frac{\bar{x}}{b} - 1 \quad \text{and} \quad \eta = \frac{\bar{y}}{a} - 1, \quad (7)$$

then linear shape functions, described by (19) in Ex. 11.9, assume the following form:

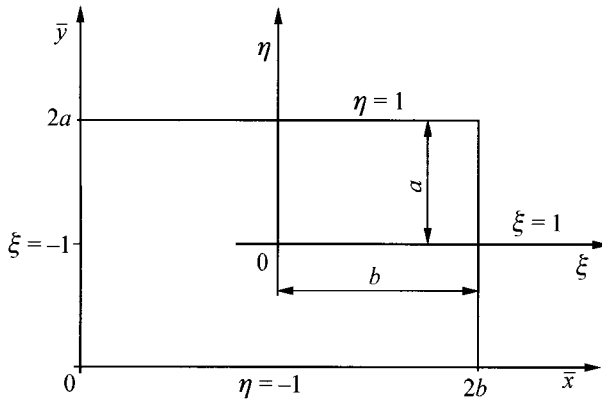


Fig. 22.6. Local (\bar{x}, \bar{y}) and natural (ξ, η) coordinate systems

$$\begin{aligned}
 N_1^e &= \frac{1}{4}(1-\xi)(1-\eta), \\
 N_2^e &= \frac{1}{4}(1+\xi)(1-\eta), \\
 N_3^e &= \frac{1}{4}(1+\xi)(1+\eta), \\
 N_4^e &= \frac{1}{4}(1-\xi)(1+\eta).
 \end{aligned} \tag{8}$$

c. Two-dimensional triangular elements

Linear shape functions for a triangular element are defined by (7) in Ex. 11.9. Natural (area) coordinate system is presented in Fig. 22.7.

By connecting point $P = P(x, y)$ with the vertices of triangle 123, three smaller triangles are obtained whose surface areas are A_1 , A_2 and A_3 (Fig. 22.7). Natural coordinate system (ξ, η, ζ) is defined as follows:

$$\begin{aligned}
 L_1 &= \xi = \frac{A_1}{A^e}, \\
 L_2 &= \eta = \frac{A_2}{A^e}, \\
 L_3 &= \zeta = \frac{A_3}{A^e},
 \end{aligned} \tag{9}$$

where $A^e = A_1 + A_2 + A_3$ is the area of the whole triangle 123 (Fig. 22.7).

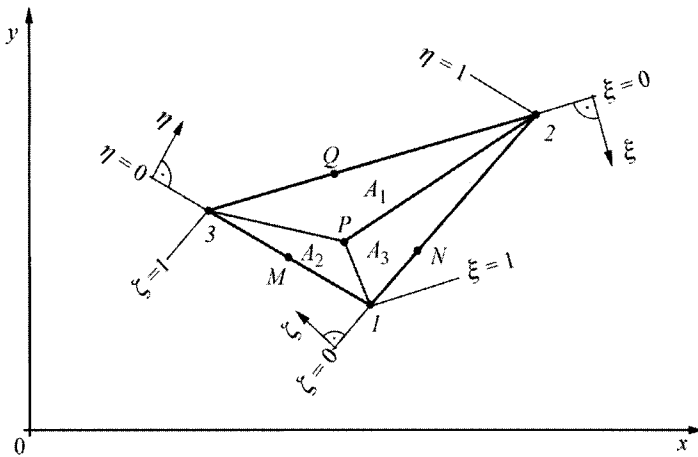


Fig. 22.7. Natural (area) coordinate system

Only two of the natural coordinates ξ, η, ζ are linearly independent, since

$$\frac{A_1}{A^e} + \frac{A_2}{A^e} + \frac{A_3}{A^e} = \frac{A^e}{A^e} = 1 = \xi + \eta + \zeta. \quad (10)$$

From (10) it follows that coordinate ζ , for example, can be expressed by functions ξ and η

$$\zeta = 1 - \xi - \eta. \quad (11)$$

All three natural coordinates change at interval $[0,1]$. If point P , which lies inside the element, is moved to node I , then $A_1 = A_{123}^e$ (Fig. 22.7) and natural coordinates equal $\xi = 1$, $\eta = 0$ and $\zeta = 0$.

If point P becomes identical with point Q , which shifts along side 23 , then $A_1 = 0$, $A_2 \neq 0$, $A_3 \neq 0$ and the respective natural coordinates are $\xi = 0$, $\eta \neq 0$ and $\zeta \neq 0$.

Similarly, when point P becomes identical with point M , which shifts along side 13 , then the natural coordinates are $\xi \neq 0$, $\eta = 0$ and $\zeta \neq 0$.

If shape functions that interpolate temperature distribution inside the element are linear, then

$$\begin{aligned} N_1^e &= L_1 = \xi, \\ N_2^e &= L_2 = \eta, \\ N_3^e &= L_3 = \zeta. \end{aligned} \quad (12)$$

Between the natural coordinates ξ , η and ζ and global coordinates x , y and z the following relationships exist

$$\begin{aligned}
x &= \xi x_1 + \eta x_2 + \zeta x_3, \\
y &= \xi y_1 + \eta y_2 + \zeta y_3, \\
1 &= \xi + \eta + \zeta.
\end{aligned} \tag{13}$$

Once the equation system (13) is solved with respect to ξ , η and ζ , one gets

$$\begin{aligned}
\xi &= N_1^e = \frac{1}{2A_{123}^e} (a_1^e + b_1^e x + c_1^e y), \\
\eta &= N_2^e = \frac{1}{2A_{123}^e} (a_2^e + b_2^e x + c_2^e y), \\
\zeta &= N_3^e = \frac{1}{2A_{123}^e} (a_3^e + b_3^e x + c_3^e y),
\end{aligned} \tag{14}$$

where $2A_{123}^e$ is defined by (5) in Chap. 11. Coefficients a_1^e , a_2^e , a_3^e , b_1^e , b_2^e , b_3^e , c_1^e , c_2^e , c_3^e are described by (8) in Chap. 11. The superscript e means that the quantities refer to a single element e .

Natural coordinates are introduced with an aim to simplify the calculation of surface integrals by means of the Gauss-Legendre quadratures method.

Only linear shape functions were analyzed. Analogically, the same procedure applies in the case of higher degree shape functions, for example quadratic or cubic [12, 21].

Exercise 22.6 Coordinate System Transformations and Integral Calculations by Means of the Gauss-Legendre Quadratures

Discuss the transformation of coordinate systems for arbitrarily-shaped tetragonal and triangular elements and the calculation of integrals by means of the Gauss-Legendre quadratures.

Solution

In Chap. 11, the integrals that occur in the coefficients of conduction matrixes and also other integrals of an algebraic equation for i -node are analytically calculated. This is possible for rectangular or triangular elements. If a region is divided into arbitrary quadrilaterals, then the analytical calculation of the integrals becomes rather problematic. In large commercial

programs, integrals are usually calculated numerically by means of the Gauss-Legendre quadratures. For this purpose, an arbitrarily-chosen quadrilateral is transformed in the coordinate system (x,y) into the, so called, model element whose dimensions are 2×2 in the new coordinate system (ξ,η) . The model is a square: $-1 \leq \xi \leq 1$, $-1 \leq \eta \leq 1$.

Coordinate transformations are only applied in order to calculate the integrals. The transformation of element B is shown in Fig. 22.8. After the transformation of coordinates (x,y) , the elements of integration in the new coordinate system (ξ,η) become more complex; in effect, therefore, a numerical method, usually the Gauss-Legendre method, is applied to calculate these integrals.

The real element B in the system (x,y) is transformed into the model element in the system (ξ,η) by means of the transformation

$$\begin{aligned} x &= \sum_{j=1}^m x_j^e N_j^e(\xi, \eta), \\ y &= \sum_{j=1}^m y_j^e N_j^e(\xi, \eta), \end{aligned} \quad (1)$$

where $N_j^e(\xi, \eta)$ is the shape function in the model element.

The examples of such transformation are (6) and (13) in Ex. 22.5.

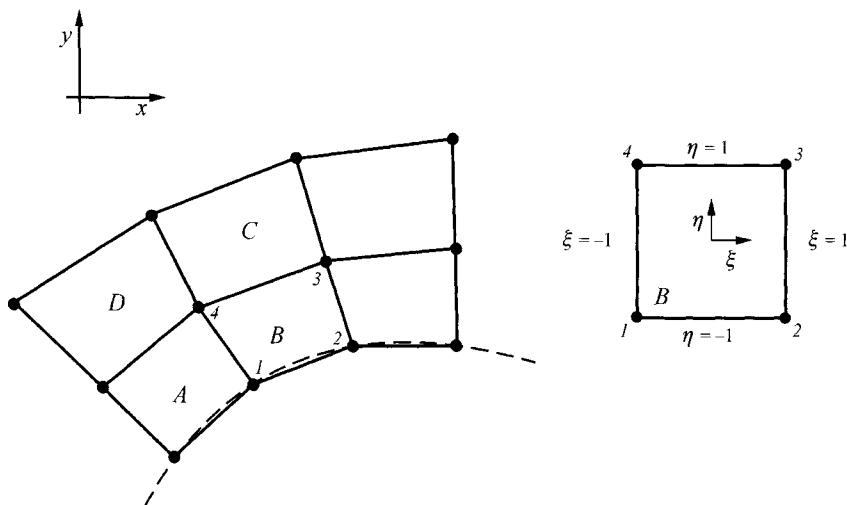


Fig. 22.8. Transformation of an arbitrary tetragonal element B in the Cartesian coordinate system (x,y) into a quadratic model element in the coordinate system (ξ,η)

Temperature distribution in element e is expressed as

$$T^e \equiv T^e(x, y) = \sum_{j=1}^n T_j^e N_j^e(x, y), \quad (2)$$

where n is the number of nodes in element e .

Natural number m , which occurs in (1) does not have to be equal to number n in (2). Depending on the relations between m and n , the elements can be divided into

- *subparametric* ($m < n$), approximation order of coordinates x and y is lower than the approximation order of temperature (in the general case of a dependent variable),
- *isoparametric* ($m = n$), approximation orders of coordinates x and y and temperature are identical,
- *superparametric* ($m > n$), approximation order of coordinates x and y is higher than the approximation order of temperature.

Most frequently, the isoparametric elements are used, for which $m = n$.

Next, the transformation of coordinates will be discussed in greater detail. The quantities, which should be transformed are

$$N_j^e(x, y), \quad \frac{\partial N_j^e}{\partial x}, \quad \frac{\partial N_j^e}{\partial y} \quad \text{and} \quad dA = dx dy. \quad (3)$$

They occur in integrals, which result from the application of FEM. For instance, the coefficients of conduction matrixes $K_{c,ij}^e$ ((26), Chap. 11) are formulated as follow:

$$K_{c,ij}^e = \int_{\Omega^e} \left(\lambda_x \frac{\partial N_i^e}{\partial x} \frac{\partial N_j^e}{\partial x} + \lambda_y \frac{\partial N_i^e}{\partial y} \frac{\partial N_j^e}{\partial y} \right) dx dy. \quad (4)$$

It is easy to express quantity $N_j^e(x, y)$ in functions ξ and η once the (1) is allowed for. The derivatives from the shape function are calculated in the following way:

$$\frac{\partial N_i^e}{\partial \xi} = \frac{\partial N_i^e}{\partial x} \frac{\partial x}{\partial \xi} + \frac{\partial N_i^e}{\partial y} \frac{\partial y}{\partial \xi}, \quad (5)$$

$$\frac{\partial N_i^e}{\partial \eta} = \frac{\partial N_i^e}{\partial x} \frac{\partial x}{\partial \eta} + \frac{\partial N_i^e}{\partial y} \frac{\partial y}{\partial \eta}. \quad (6)$$

Equations (5) and (6) can be written in the matrix form

$$\begin{Bmatrix} \frac{\partial N_i^e}{\partial \xi} \\ \frac{\partial N_i^e}{\partial \eta} \end{Bmatrix} = \begin{bmatrix} \frac{\partial x}{\partial \xi} & \frac{\partial y}{\partial \xi} \\ \frac{\partial x}{\partial \eta} & \frac{\partial y}{\partial \eta} \end{bmatrix} \begin{Bmatrix} \frac{\partial N_i^e}{\partial x} \\ \frac{\partial N_i^e}{\partial y} \end{Bmatrix}, \quad (7)$$

where the square matrix with dimensions 2×2 is a Jacobian determinant

$$\mathbf{J} = \begin{bmatrix} \frac{\partial x}{\partial \xi} & \frac{\partial y}{\partial \xi} \\ \frac{\partial x}{\partial \eta} & \frac{\partial y}{\partial \eta} \end{bmatrix}. \quad (8)$$

The transformation of coordinates is unique when the Jacobian \mathbf{J} is not singular, i.e. when Jacobian determinant is other than zero at every point (ξ, η)

$$J \equiv \det \mathbf{J} = \frac{\partial x}{\partial \xi} \frac{\partial y}{\partial \eta} - \frac{\partial x}{\partial \eta} \frac{\partial y}{\partial \xi} \neq 0. \quad (9)$$

Derivatives from integral (4) are determined from the transformation of (7)

$$\begin{Bmatrix} \frac{\partial N_i^e}{\partial x} \\ \frac{\partial N_i^e}{\partial y} \end{Bmatrix} = [\mathbf{J}]^{-1} \begin{Bmatrix} \frac{\partial N_i^e}{\partial \xi} \\ \frac{\partial N_i^e}{\partial \eta} \end{Bmatrix}. \quad (10)$$

The required derivatives for the calculation of the Jacobian determinant (9) are obtained after the differentiation of

$$\begin{aligned} \frac{\partial x}{\partial \xi} &= \sum_{j=1}^m x_j \frac{\partial N_j^e}{\partial \xi}, \\ \frac{\partial y}{\partial \xi} &= \sum_{j=1}^m y_j \frac{\partial N_j^e}{\partial \xi}, \end{aligned} \quad (11)$$

$$\begin{aligned} \frac{\partial x}{\partial \eta} &= \sum_{j=1}^m x_j \frac{\partial N_j^e}{\partial \eta}, \\ \frac{\partial y}{\partial \eta} &= \sum_{j=1}^m y_j \frac{\partial N_j^e}{\partial \eta}. \end{aligned} \quad (12)$$

The element of surface area $dxdy$ equals

$$dxdy = \det \mathbf{J} d\xi d\eta. \quad (13)$$

From (10) or directly from the solution of the equation systems (5) and (6), one has

$$\frac{\partial N_i^e}{\partial x} = \frac{1}{\det \mathbf{J}} \left[\frac{\partial y}{\partial \eta} \frac{\partial N_j^e}{\partial \xi} - \frac{\partial y}{\partial \xi} \frac{\partial N_j^e}{\partial \eta} \right], \quad (14)$$

$$\frac{\partial N_i^e}{\partial y} = \frac{1}{\det \mathbf{J}} \left[\frac{\partial x}{\partial \xi} \frac{\partial N_i^e}{\partial \eta} - \frac{\partial x}{\partial \eta} \frac{\partial N_i^e}{\partial \xi} \right]. \quad (15)$$

Integral (4) can be transformed into a new coordinate system when the derived relationships are applied. The first component of this integral can be transformed by means of the (13)–(15) into a form

$$\begin{aligned} I^e &= \int_{\Omega^e} \left(\lambda_x \frac{\partial N_i^e}{\partial x} \frac{\partial N_j^e}{\partial x} \right) dxdy = \\ &= \int_{-1}^1 \int_{-1}^1 \frac{\lambda_x}{\det \mathbf{J}} \left(\frac{\partial y}{\partial \eta} \frac{\partial N_i^e}{\partial \xi} - \frac{\partial y}{\partial \xi} \frac{\partial N_i^e}{\partial \eta} \right) \left(\frac{\partial y}{\partial \eta} \frac{\partial N_j^e}{\partial \xi} - \frac{\partial y}{\partial \xi} \frac{\partial N_j^e}{\partial \eta} \right) d\xi d\eta. \end{aligned} \quad (16)$$

One can see, therefore, that after the transformation of coordinates, the subintegral expressions are more complex in the new coordinate system (ξ, η) than they are in the coordinate system (x, y) . These integrals are usually numerically calculated using the Gauss-Legendre quadrature [1, 3, 11–17, 21]. If the subintegral function is denoted by $F(\xi, \eta)$, one can calculate the integrals in the new coordinate system by means of a relatively simple formulas.

a. One-dimensional elements

The integral is calculated by means of formula

$$I = \int_{-1}^1 F(\xi) d\xi = \sum_{i=1}^n w_i F(\xi_i), \quad (17)$$

where ξ_i are the Gaussian point coordinates (Fig. 22.9).

Coordinates ξ_i are the zeros of Legendre polynomials [13]. Coordinates ξ_i and weights w_i , which occur in (17) are compiled in Table 22.1.

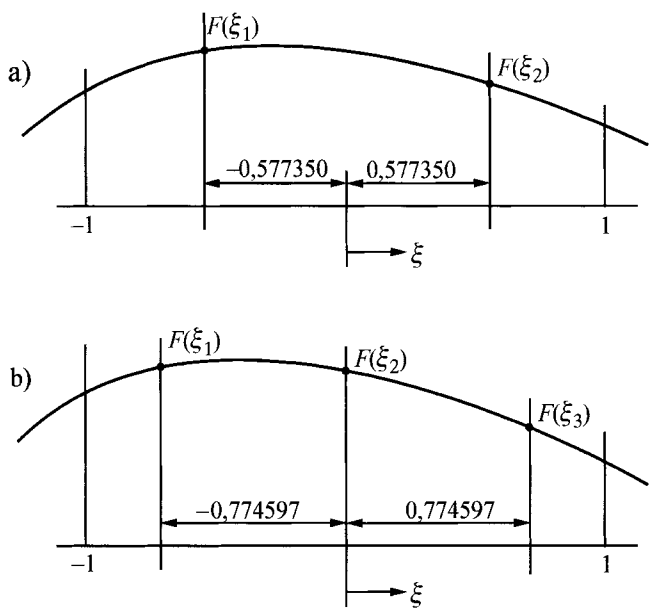


Fig. 22.9. The location of Gaussian points during the calculation of a one-dimensional integral: a) $n = 2$, b) $n = 3$

Table 22.1. Legendre polynomials and the coefficients of the Gauss-Legendre quadratures

n	Nodes ξ_i	Weight coefficients w_i
1	0,0	2,0
2	$\pm 0,577350$	1,0
3	0,0	$8/9 = 0,888 \dots$
	$\pm 0,774597$	$5/9 = 0,555 \dots$
4	$\pm 0,339982$	0,652145
	$\pm 0,861136$	0,347855
5	0,0	0,568889
	$\pm 0,538469$	0,478629
	$\pm 0,906180$	0,236927

The integration by means of the Gaussian quadratures yields accurate results for n integration points, when $F(\xi)$ is the polynomial of degree $2n-1$ or lower. In general, the larger the number of Gaussian points n , the more accurate the calculation of integral (17) is. Now we will discuss the approximate calculation of two-dimensional integrals for tetragonal and triangular elements.

b. Tetragonal elements

Formulas for the calculation of an integral in a two-dimensional region are used to determine integrals for quadrilateral elements.

$$\begin{aligned}
 I &= \int_{-1}^1 \int_{-1}^1 F(\xi, \eta) d\xi d\eta = \int_{-1}^1 \left[\sum_{j=1}^n w_j F(\xi_j, \eta) \right] d\eta = \\
 &= \sum_{k=1}^n w_k \left[\sum_{j=1}^n w_j F(\xi_j, \eta_k) \right] = \sum_{j=1}^n \sum_{k=1}^n w_j w_k F(\xi_j, \eta_k),
 \end{aligned}
 \tag{18}$$

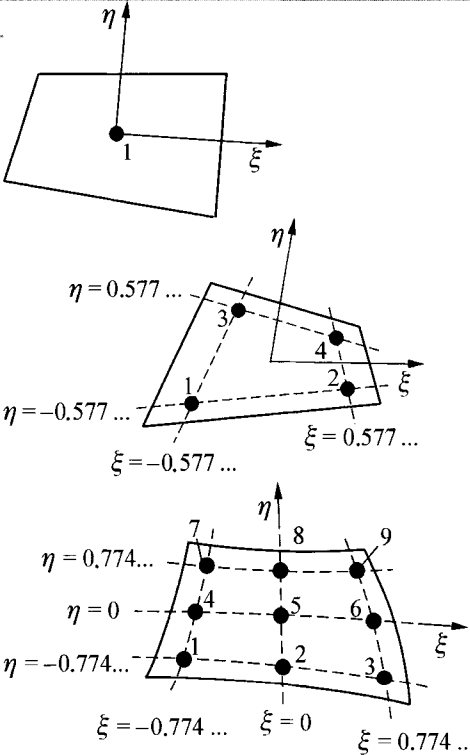
where n is the Gaussian point number in a single direction. For $n = 2$, the integral (18) can be written as follows:

$$I = w_1 w_1 F(\xi_1, \eta_1) + w_1 w_2 F(\xi_1, \eta_2) + w_2 w_1 F(\xi_2, \eta_1) + w_2 w_2 F(\xi_2, \eta_2), \tag{19}$$

where the coordinates of Gaussian point are $\xi_i, \eta_i = \pm 1/3^{1/2} = \pm 0.57735$ and $w_1^2 = w_1 w_2 = w_2^2 = 1$.

Table 22.2. Calculating integrals in a quadrilateral region by means of (20)

m	i	ξ_i	η_i	w_i
1	1	0	0	4
	2	0	0	4
	3	0	0	4
	4	0	0	4
4	1	$-1/3^{1/2}$	$-1/3^{1/2}$	1
	2	$+1/3^{1/2}$	$-1/3^{1/2}$	1
	3	$-1/3^{1/2}$	$+1/3^{1/2}$	1
	4	$+1/3^{1/2}$	$+1/3^{1/2}$	1
9	1	$-(3/5)^{1/2}$	$-(3/5)^{1/2}$	25/81
	2	0	$-(3/5)^{1/2}$	40/81
	3	$+(3/5)^{1/2}$	$-(3/5)^{1/2}$	25/81
	4	$-(3/5)^{1/2}$	0	40/81
	5	0	0	64/81
	6	$+(3/5)^{1/2}$	0	40/81
	7	$-(3/5)^{1/2}$	$+(3/5)^{1/2}$	25/81
	8	0	$+(3/5)^{1/2}$	40/81
	9	$+(3/5)^{1/2}$	$+(3/5)^{1/2}$	25/81



One can see, therefore, that once the numeration of nodes $i = j + (k - 1)n$ is introduced, the integral (18) can be written in the form

$$I = \sum_{i=1}^m F(\xi_i, \eta_i) w_i, \quad (20)$$

where $m = n^2$, $\xi_i = \alpha_j$, $\eta_i = \alpha_k$ and $w_i = w_j w_k$. Quantities α_j and w_j denote coordinates ξ_j and weights w_j , respectively, compiled in Table 22.2 and are used to calculate two-dimensional integrals.

c. Triangular elements

To calculate the integral, coordinates (x, y) are transformed into area coordinates L_1 and L_2 , which are linearly independent, since once we account for the (11) from Ex. 22.5, coordinate L_3 can be calculated from formula

$$L_3 = 1 - L_1 - L_2.$$

By allowing for equation

$$\begin{Bmatrix} \frac{\partial N_i^e}{\partial x} \\ \frac{\partial N_i^e}{\partial y} \end{Bmatrix} = [J]^{-1} \begin{Bmatrix} \frac{\partial N_i^e}{\partial L_1} \\ \frac{\partial N_i^e}{\partial L_2} \end{Bmatrix}, \quad (21)$$

where

$$[J] = \begin{bmatrix} \frac{\partial x}{\partial L_1} & \frac{\partial y}{\partial L_1} \\ \frac{\partial x}{\partial L_2} & \frac{\partial y}{\partial L_2} \end{bmatrix}, \quad (22)$$

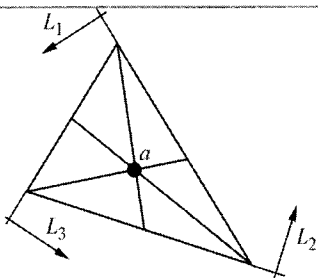
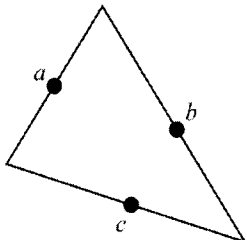
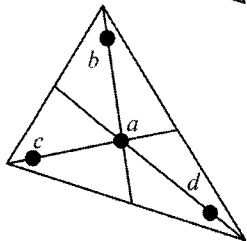
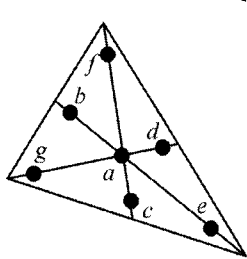
surface integral I for a triangular element is calculated from formula

$$I = \int_0^1 \int_0^{1-L_1} F(L_1, L_2, L_3) dL_2 dL_1 \approx \sum_{i=1}^m F(L_{1,i}, L_{2,i}, L_{3,i}) w_i \quad (23)$$

The locations of integration points and weight coefficients for the triangular element [1, 3, 11, 12, 14, 15, 21] are compiled in Table 22.3.

In both, Chap. 11 and this chapter, the discussion was limited to one and two-dimensional steady-state and transient heat conduction problems. Three-dimensional problems are solved analogically, in keeping with the rules that were applied in the examples of two-dimensional problems, which were discussed above.

Table 22.3. The location of integration and weight points for a triangular element

Integration points number	Point location	Error	Point L_1, L_2, L_3	Coordinates L_1, L_2, L_3	Weights w_i
1		$R = O(h^2)$	a	$\frac{1}{3}, \frac{1}{3}, \frac{1}{3}$	1
3		$R = O(h^3)$	a b c	$\frac{1}{2}, \frac{1}{2}, 0$ $0, \frac{1}{2}, \frac{1}{2}$ $\frac{1}{2}, 0, \frac{1}{2}$	$\frac{1}{3}$ $\frac{1}{3}$ $\frac{1}{3}$
4		$R = O(h^4)$	a b c d	$\frac{1}{3}, \frac{1}{3}, \frac{1}{3}$ $0, 6; 0, 2; 0, 2$ $0, 2; 0, 6; 0, 2$ $0, 2; 0, 2; 0, 6$	$-\frac{27}{48}$ $\frac{25}{48}$ $\frac{25}{48}$
7		$R = O(h^6)$	a b c d e f g	$\frac{1}{3}, \frac{1}{3}, \frac{1}{3}$ $\alpha_1, \beta_1, \beta_1$ $\beta_1, \alpha_1, \beta_1$ $\beta_1, \beta_1, \alpha_1$ $\alpha_2, \beta_2, \beta_2$ $\beta_2, \alpha_2, \beta_2$ $\beta_2, \beta_2, \alpha_2$	0,2250000000 $0,1323941527$ $0,1259391805$

Constants $\alpha_1, \alpha_2, \beta_1$ and β_2 are $\alpha_1 = 0.0597158717, \beta_1 = 0.4701420641, \alpha_2 = 0.7974269853, \beta_2 = 0.1012865073$.

Exercise 22.7 Calculating Temperature in a Complex-Shape Fin by Means of the ANSYS Program

Oval pipes with an attached aluminum plate-fins, $\delta_z = 0.08$ mm thick are used in car radiators [19]. Due to the division of plate-fin into fictions (equivalent) fins, temperature distribution in the entire lamella can be determined when temperature distribution only in half of the fin is analyzed [19].

The maximum length of the pipe diameter is $d_{\max} = 11.82$ mm, while the minimum $d_{\min} = 6.35$ mm (Fig. 22.10). The height of the fin half section is $h = 9.25$ mm, while the width $s = 17.0$ mm. Initial temperature of the fin is $T_0 = 20^\circ\text{C}$. The temperature of surroundings is also $T_{cz} = 20^\circ\text{C}$. At an instant $t = 0$ s, the fin base temperature increases by a step from temperature $T_0 = 20^\circ\text{C}$ to $T_p = 95^\circ\text{C}$.

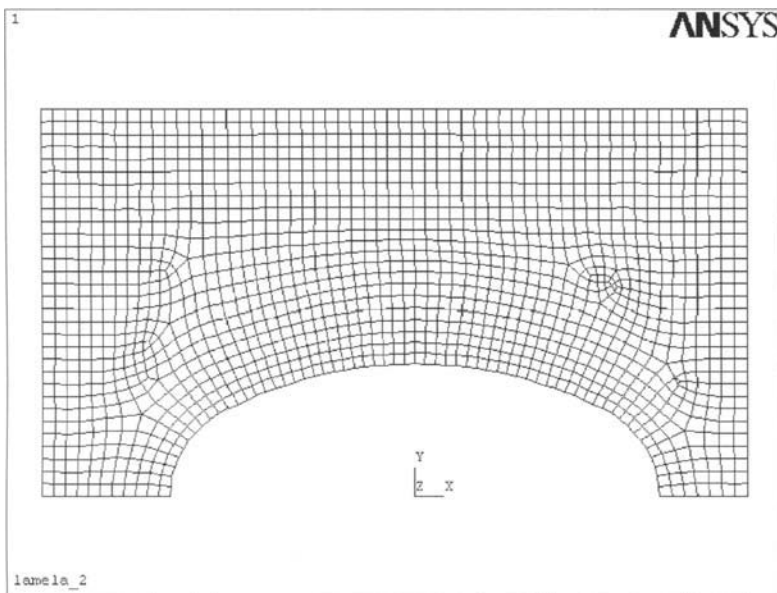


Fig. 22.10. The division of 1/4 of a plate-fin into finite elements

Determine transient fin temperature distribution at time $t_1 = 1.0$ s and $t_1 = 0.2$ s and temperature transient in the upper-left fin corner in the function of time. Heat transfer coefficient on the fin surface is $\alpha = 75$ W/(m²·K). Heat is given off by the fin to surroundings through the lateral surfaces and through the left lateral front face. The upper and right-hand-side surfaces are thermally insulated. Straight sections of the fin base are also thermally insulated due to the symmetry of the temperature field with respect to the

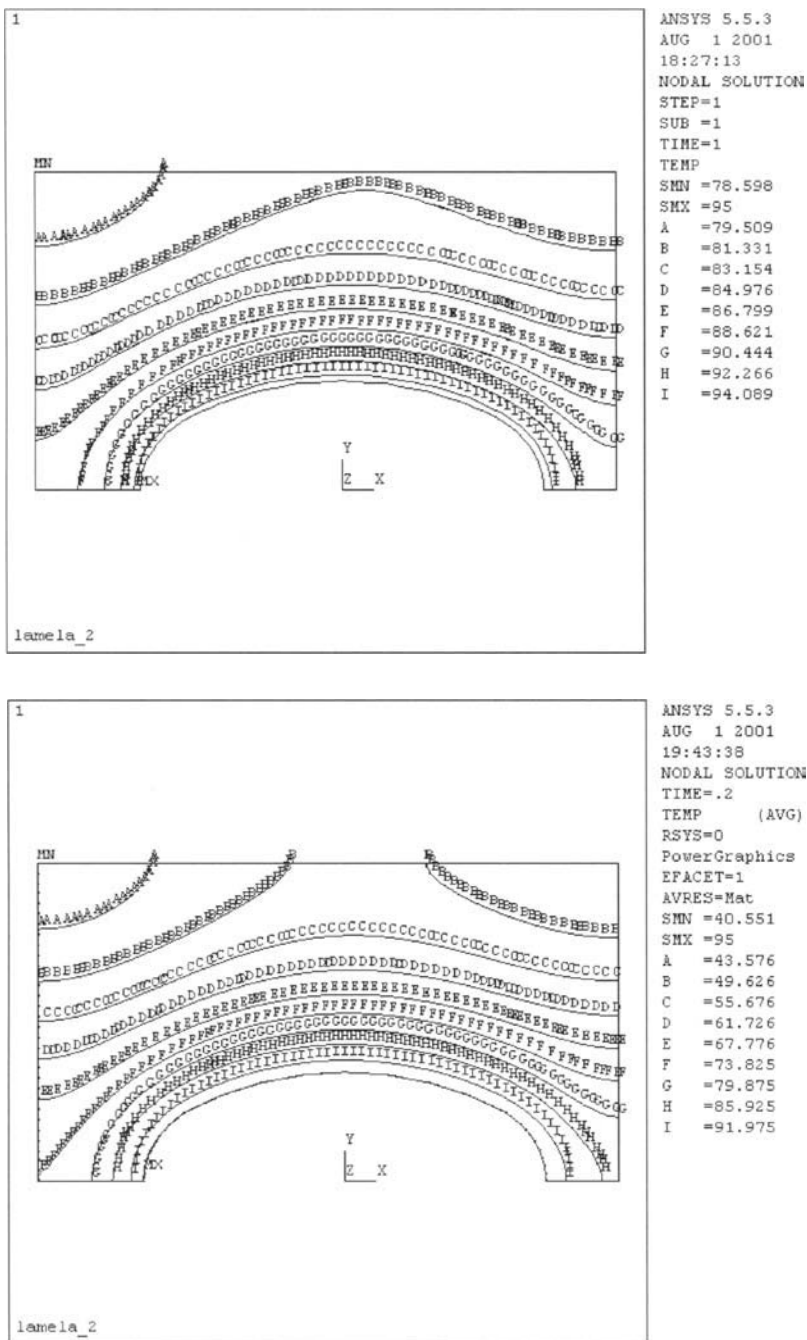


Fig. 22.11. Distribution of isotherms in a fin: a) $t_1 = 1.0$ s, b) $t_2 = 0.2$ s

horizontal axis of the pipe cross-section. The pipe axis is at a distance of 9 mm from the left side. Assume for the calculation that the aluminium has the following thermo-physical properties: $\lambda = 207 \text{ W/(m}\cdot\text{K)}$, $c = 879 \text{ J/(kg}\cdot\text{K)}$ and $\rho = 2696 \text{ kg/m}^3$.

Solution

Due to the symmetry of the temperature field in the fin shown in Fig. 22.10, the temperature distribution will be determined only for one-half of the fin, which is in thickness $\delta_z/2 = 0.04 \text{ mm}$. The back surface of the fin is thermally insulated, while the heat is given off to surroundings on the fin's front surface.

A quarter of the conventional fin was divided into 1500 elements (Fig. 22.10). Temperature was determined in 3198 nodes. Only one finite element is located at $\delta/2 = 0.04 \text{ mm}$. Calculations were carried out by means of the ANSYS program. The isotherm history on the lateral fin surface at time $t_1 = 1.0 \text{ s}$ is presented in Fig. 22.11a, while at time $t_2 = 0.2 \text{ s}$ in Fig. 22.11b. It is evident that the fin quickly becomes heated and at an instant $t_1 = 1.0 \text{ s}$ temperature distribution is almost steady-state.

Temperature history for the upper left-hand-corner of the fin (point *MN* in Fig. 22.11) is presented in Table 22.4 and in Fig. 22.12.

Steady-state temperature at the point *MN* is $T_{MN} = 78.958^\circ\text{C}$. It is clear, therefore, that already after time $t = 1.2 \text{ s}$ temperature differs by

Table 22.4. Temperature history for the upper left-hand-corner of the fin (point *MN*)

Entry no.	Time $t \text{ [s]}$	Temperature $[\text{°C}]$	Entry no.	Time $t \text{ [s]}$	Temperature $[\text{°C}]$
1	0.00	20.00	11	1.00	77.81
2	0.10	23.78	12	1.10	78.17
3	0.20	40.55	13	1.20	78.30
4	0.30	54.85	14	1.30	78.41
5	0.40	63.93	15	1.40	78.49
6	0.50	69.55	16	1.50	78.53
7	0.60	73.03	17	1.60	78.56
8	0.70	75.18	18	1.70	78.57
9	0.80	76.50	19	1.80	78.58
10	0.90	77.59	20	1.90	78.59

$$e = \frac{78.304 - 78.598}{78.598} \cdot 100 = -0.37\%$$

From the steady-state temperature.

Fin temperature quickly reaches the steady-state, since for the aluminum thermal diffusivity is very high and is $a = \lambda/(c\rho) = 207/(879 \cdot 2696) = 8.735 \cdot 10^{-5} \text{ m}^2/\text{s}$.

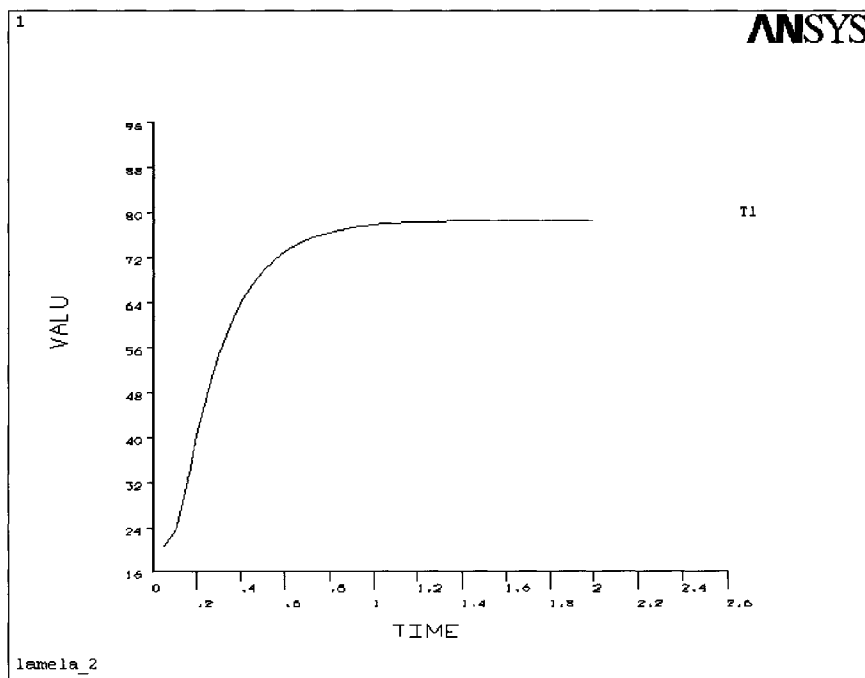


Fig. 22.12. Temperature history in the upper left-hand-corner of a fin (point *MN* in Fig. 22.11)

Literature

1. Akin JE (1998) Finite Elements for Analysis and Design. Academic Press-Harcourt Brace & Company, London
2. Anderson JD (1995) Computational Fluid Dynamics. The Basics with Applications. McGraw-Hill, New York
3. Bathe KJ (1996) Finite Element Procedures., Prentice Hall, Upper Saddle River
4. Burnett DS (1988) Finite Element Analysis. Addison-Wesley Publishing Company, Reading

5. Champion ER (1992) *Finite Element Analysis in Manufacturing Engineering*. McGraw-Hill, New York
6. Ergatoudis I, Irons BM, Zienkiewicz OC (1968) Curved isoparametric quadrilateral elements for finite element analysis. *Int. J. of Solids and Structures* 4: 31-42
7. Fletcher CAJ (1984) *Computational Galerkin Methods*. Springer, New York
8. Gresho PM, Sani RL, Engelman MS (2000) *Incompressible Flow and the Finite Element Method*. Wiley, Chichester
9. Irons BM (1966) Engineering Application of numerical integration in stiffness method. *AIAA J.* 4(11): 2035-2037
10. Lewis E, Ward JP (1991) *Finite Element Method. Principles and Applications*. Addison-Wesley, Wokingham
11. Logan DL (1997) *A First Course in the Finite Element Method Using Algor*. PWS Publishing Company, Boston
12. Moaveni S (1999) *Finite Element Method. Theory and Applications with ANSYS*. Prentice Hall, Upper Saddle River
13. Ralston A (1965) *A First Course in Numerical Analysis*. McGraw-Hill, New York
14. Reddy JN, Gartling DK (1994) *The Finite Element Method in Heat Transfer and Fluid Dynamics*. CRC Press, Boca Raton
15. Segerlind LJ (1984) *Applied Finite Element Analysis*. Wiley, New York
16. Stroud AH, Secrest D (1966) *Gaussian Quadrature Formulas*. Prentice Hall, Englewood Cliffs
17. Szmelter J (1980) *Computer Programming Methods in Mechanical Engineering* (in Polish). PWN, Warsaw
18. Taig IC (1961) *Structural Analysis by the Matrix Displacement Method*. English Electric Aviation Report S017
19. Taler D (2002) *Theoretical and experimental analysis of heat exchangers with extended surfaces*. Ph.D. thesis, Univ. of Science and Technology
20. Taylor C, Hughes TG (1981) *Finite Element Programming of the Navier-Stokes Equations*. Pineridge Press Ltd, Swansea
21. Zienkiewicz OC, Taylor RL (2000) *The Finite Element Method*. Ed. 5. Butterworth-Heinemann, Oxford